

POLR2A Drives Tumor Cell Aggressive in Both *VHL* and *PBRM1* Mutation Renal-Cell Carcinoma

Linyan Chai

Xi'an Jiaotong University

Zhengguo Qiu

Xi'an Jiaotong University

Xiaozhi Zhang

Xi'an jiaotong university

Rong Li

Xi'an jiaotong university

Yao Wang

Xi'an jiaotong university

Kefeng Wang (✉ 17749028125@stu.xjtu.edu.cn)

Xi'an jiaotong university <https://orcid.org/0000-0003-4394-1225>

Research Article

Keywords: RCC, POLR2A, tumor growth, mutation

Posted Date: November 3rd, 2021

DOI: <https://doi.org/10.21203/rs.3.rs-1039666/v1>

License:   This work is licensed under a Creative Commons Attribution 4.0 International License.

[Read Full License](#)

Abstract

Background: Loss of *VHL* always results in the loss of *PBRM1* and causes aggressive clear cell renal cell carcinoma. However, *VHL* mutation was not significantly associated with worse survival, and *PBRM1* modulate the tumor behavior is not clear. Thus, exploration of key molecules promoting the tumor aggressive is urgent in both *VHL* and *PBRM1* RCC patient.

Methods and results: POLR2A was screened out by analyzing The Cancer Genome Atlas mutation data. Gene Set Enrichment Analysis results showed that E2F, G2M, and mTOR1 pathways were all altered in response to POLR2A high expression. Furthermore, In vitro, knockdown of POLR2A in 769-P and 786-O cells resulted in cell growth arrest and cell cycle blockade compared to control cells, the mechanism though decreasing cyclin D1-CDK4 axis. In vivo results were confirmed 786-O cells in which POLR2A expression was silenced, exhibited tumor growth inhibited compared to control group.

Conclusions: POLR2A was the key protein after *VHL* and *PBRM1* mutations in RCC, inhibition of POLR2A crippled cell viability and proliferation in vivo and in vitro, We anticipate POLR2A represents a novel candidate for RCC treatment.

Background

Clear cell renal cell carcinoma (ccRCC) is a type of kidney cancer that displays a variety of clinical behaviors[1, 2]. Approximately 85-90% of renal cell carcinoma is ccRCC, and approximately 403,262 new cases of RCC occurred, with an estimated 175,098 deaths worldwide in 2018[1]. The prognosis of metastatic ccRCC is poor, and the 5-year survival rate is <10% after diagnosis[3].

3p loss occurs in 70% of ccRCC patients and leads to the loss of tumor suppressor genes Von Hippel-Lindau (*VHL*), Polybromo-1 (*PBRM1*), Set domain-containing 2 (*SETD2*), and BRCA1-associated protein-1 (*BAP1*)[4]. Subsequently, the loss of *VHL* always results in the loss of *PBRM1* and causes aggressive ccRCC[5–7]. The *VHL* gene, which encodes a tumor suppressor, the VHL protein, is highly mutated in ccRCC, and its mutation rate is approximately 47%[8]. The function of the VHL protein is to participate in the degradation of hypoxia-inducible factor (HIF) protein[9]. *VHL* mutation leads to VHL protein loss of function and causes HIF protein accumulation[10]; furthermore, the HIF protein activates the mammalian target of rapamycin (mTOR) and vascular endothelial growth factor (VEGF) signaling pathways[11]. To date, sunitinib and pazopanib (inhibitors of the VEGF/VEGFR pathway) and everolimus and temsiromus (inhibitors of mTOR kinase) have been used as clinical treatments for ccRCC patients[3]. However, neither *VHL* mutation nor deletion is significantly associated with worse survival in ccRCC patients according to Young et al's report[9].

PBRM1, which is involved in a crucial step in ccRCC carcinogenesis, encodes the BRG1-associated factor 180 (BAF180) protein, a subunit of the nucleosome remodeling complex[12]. In ccRCC, *PBRM1* has an up to 40% mutation rate and a highly methylated gene promoter[8]. Loss of BAF180 disrupts the nucleosome remodeling complex and causes aggressive RCC, prostate cancer, and non-small cell lung

cancer[13–16]. In Kapur et al's. report, BAF180 is not an independent predictor of outcome in ccRCC. *PBRM1* mutations have been associated with high angiogenic gene expression and appear to be able to predict the clinical benefit of targeted therapy[17]. Meanwhile, there are studies about *PBRM1*'s effect on immune inhibitor clinical therapy. However, other reports in the literature present a contrary conclusion about the function of *PBRM1* in immune therapy, and its mechanisms are unclear[18–20]. *VHL* and *PBRM1* are both highly mutated genes in ccRCC[3]; however, *VHL* and *PBRM1* mutations in combination exhibit aggressive pathological features in ccRCC, not alone.

In the present study, we found that *POLR2A* was lost after *VHL* and *PBRM1* mutations. *POLR2A*, a subunit of the RNA polymerase II complex, has polymerase activity in mRNA synthesis[21]. To the best of our knowledge, *POLR2A* has been reported to mutation in many human cancers, including human triple-negative breast cancer, hepatocellular carcinoma, and human colorectal cancers[22–25]. Notably, the loss of *POLR2A* leads to a decreased abundance of RNA polymerase II in *TP53*[−]/*POLR2A*[−] tumor cells, and *TP53*[−]/*POLR2A*[−] tumor cells are more sensitive to α -amanitin (*POLR2A* is specifically inhibited by α -amanitin) than unaltered normal cells[25]. However, the role of *POLR2A* in RCC is not well known. The role of *POLR2A* was analyzed in our study, and we found that *POLR2A* may be a potential target for the treatment of ccRCC growth.

Methods

Patients & clinical samples

Transcriptome (count and FPKM value) information and mutational data of 539 ccRCC patients were downloaded from The Cancer Genome Atlas (TCGA, <https://www.cancer.gov/tcga>) database. Variance stabilizing transformation (VST) was used to normalize the data sets, and then, low-value genes were removed using heterogeneity analysis. According to the *VHL* gene, the wild-type *VHL* (*VHL*^{WT}) and mutant *VHL* (*VHL*^{MT}) patient groups were set, and then, by using the edgeR and clusterProfiler packages, gene set enrichment analysis (GSEA) was performed to determine significantly altered pathways between *POLR2A* Low and *POLR2A* high groups.

Cell lines and cell culture

The clear cell renal carcinoma cell lines 786-O and 769-P were purchased from American Type Culture Collection (ATCC, <https://www.atcc.org>) and maintained in RPMI medium modified (Cytiva, Shanghai, China) with 10% (v/v) fetal bovine serum (Biological Industries, Israel) at 37 °C in a humidified 5% CO₂ incubator.

Transfection

786-O and 769-P cells were cultured in 6-well dishes. After 24 h, plasmids were transfected into 786-O and 769-P cells by the Roche X-tremeGENE DNA transfection reagent (Roche Co. Ltd., Shanghai, China). Real-

time quantitative PCR and western blotting were used to verify POLR2A mRNA and protein expression, respectively.

Plasmids were purchased from Bio-company (Vigene Biosciences. Inc., Shandong, China) the sequence as follows: Sh1:CCGGGCGGAATGGAAGCACGTTAATCTCGAGATTAACGTGCTTCCATTCCGCTTTTTG;

Sh2:CCGGTGCGGAATGGAAGCACGTTAACTCGAGTTAACGTGCTTCCATTCCGCATTTTTG;

Sh3:CCGGCGACTTGAAGTGCATCTTTAACTCGAGTTAAAGATGCAGTTCAAGTCGTTTTTTG;

NCshRNA:TTCTCCGAACGTGTCACGTTTCAAGAGAACGTGACACGTTCCGGAGAATTTTTT.

RNA isolation and real-time quantitative PCR

After 48 h of transfection, total RNA from 786-O and 769-P cells was isolated using the RNA fast 200 kit (Feijie Biotech, Shanghai, China) and then reverse-transcribed using the Prime Script™ RT reagent kit (Takara Biotechnology Co. Ltd., Dalian, China). Relative gene expression was detected by SYBR Green PCR Master Mix (Takara Biotechnology Co. Ltd., Dalian, China) and calculated by the $2^{-\Delta\Delta Ct}$ method using GAPDH as a reference gene[26]. The sequences of the GAPDH and POLR2A primers were as follows:

GAPDH forward, 5'-ATGGGGAAGGTGAAGGTCGG-3',

GAPDH reverse, 5'-GACGGTGCCATGGAATTTGC-3',

POLR2A forward, 5'-GGGTGGCATCAAATACCCAGA-3',

POLR2A reverse, 5'-AGACACAGCGCAAACTTTCA-3'.

Western blot analysis

The cell lysis and western blotting protocols were described previously. Thirty micrograms of whole protein were separated by 12.5% SDS-PAGE (#PG113, Epizyme, Shanghai, China). An anti-POLR2A antibody (ABclonal, #A20363, 1:1000, Wuhai, China), anti-CDK4 antibody (Santa Cruz, #sc-23896, 1:400 Shanghai, China), anti-PCNA antibody (CST, #2586, 1:1000, Shanghai, China), anti-cyclin D1 antibody (Santa Cruz, #sc-8396, 1:200, Shanghai, China), and anti-β-actin antibody (Absin, #JB09, 1:1000, Shanghai, China) were used. The secondary antibodies were an anti-rabbit IgG (Beijing Zhongshan, #ZB-2301; 1:2,000; Beijing, China) and anti-mouse IgG (Beijing Zhongshan, #ZB-2305; 1:2000; Beijing, China).

MTT assay

A total of 4000 cells were plated in 96-well plates in triplicate for 48 h. Cell viability was quantified using 3-(4,5-dimethyl-2-thiazolyl)-2,5-diphenyl-2-H-tetrazolium bromide (MTT). The growth rate was calculated

as follows: average OD value in the POLR2A knockdown cell group/average OD value in the control group ×100%.

Clone formation assay

A total of 1000 cells were plated in 6-well plates in triplicate. After incubation for 7 days, cell colonies were visualized by crystal violet (0.5% m/v), and then, images were captured under a microscope.

Animal experiments

These experiment were approved by the institutional review board of the First Afliated Hospital of Xi'an Jiaotong University. We randomly separated 8 BALB/c nude mice (4 weeks, male) into 2 groups. These nude mice were subcutaneously injected with 3×10^6 cells (786-O control or shPOLR2A) into the left or right shoulder. tumor size and body weight were measured every 5 days for 25 days. Tumor volume was calculated using the following equation: tumor volume=length×width×height×0.523. At the end of the experiment, the animals were all euthanized, and tumor tissues were surgically excised from the nude mice.

Statistical analysis

Each experiment was repeated three times. Differences between two groups (Student's t-test) were compared by GraphPad Prism software (Version 6.0 software, GraphPad, USA), and data are shown as the mean ± SD with error bars (SEM). $P < 0.05$ was considered significant in our study.

Results

POLR2A is the hub gene after *VHL* and *PBRM1* mutations in ccRCC

To search for hub genes or representative biomarkers related to *VHL* and *PBRM1* mutations, we analyzed ccRCC TCGA data. Three hundred ninety-seven *VHL*^{WT} patients and 155 *VHL*^{MT} patients, 400 *PBRM1*^{WT} patients and 135 *PBRM1*^{MT} patients were included. Samples with no mutation or RNA-seq data from TCGA were not included in our analysis. Comparing the *VHL*^{WT} and *VHL*^{MT} ccRCC groups, we identified the top 100 differentially expressed genes in TCGA (Figure 1A, supplementary table I). The same analysis was performed between *PBRM1*^{WT} and *PBRM1*^{MT} patients (Figure 1A, supplementary table I).

Next, the hub proteins among the top 200 differentially expressed genes were used to construct a PPI network using STRING (Figure 1B). POLR2A and POLR2E proteins were the hub protein in PPI results identified (supplementary Table II). POLR2A and POLR2E both encode RNA II polymerase, and this polymerase is responsible for synthesizing messenger RNA in eukaryotes. To the best of our knowledge, POLR2A is reported to be mutated in most tumors. However, the role of POLR2A in RCC requires investigation, and we analyzed the role of the POLR2A gene in subsequent experiments.

Pathway enrichment analysis for POLR2A in ccRCC

To investigate the potential biological processes of POLR2A involved in RCC, We found that 44/50 distribution curves to be “bumpy” in POLR2A expression high-group enrichment, whereas, 6 signaling pathways were enrichment in POLR2A low expression group (Figure 2). Furthermore, we found the gene sets of “HALLMARK_MITOTIC_SPINDLE (Figure 2A),” “HALLMARK_G2M_CHECKPOINT (Figure 2B),” and “HALLMARK_E2F_TARGET (Figure 2C)” were all responsible for the high expression POLR2A in progress biological behavior of ccRCC, three tumor cell cycle control pathways.

“HALLMARK_TGF_BETA_SIGNALING (Figure 2D),” “HALLMARK_MYC_TARGETS_V2 (Figure 2E)” and “HALLMARK_PI3K_AKT_MTOR_SIGNALING (Figure 2F)” were also found existed in high POLR2A expression group, three overactivated pathways in most tumors. Figure 2 results revealed that high POLR2A was associated with increased tumor cell proliferation in ccRCC malignant progression.

POLR2A knockdown reduced RCC tumor cell growth in vitro

To confirm the cell cycle control of POLR2A on tumor cells in RCC, the 786-O and 769-P RCC cell lines with POLR2A knockdown were constructed (Figure 3A, 3B). Figure 3A shows POLR2A mRNA and protein expression after POLR2A knockdown for 48 h. The MTT assay revealed that knocking down POLR2A in 786-O and 769-P cells led to cell growth inhibition in the two cell lines compared with the negative control (Figure 3C, D). Furthermore, colony formation assays were performed using 786-O and 769-P cells. Consistently, as shown in Figure 3E, knocking down POLR2A dramatically decreased the number of colonies in 786-O and 769-P cells, indicating that the colony formation capacity of ccRCC cells was inhibited by knocking down POLR2A in tumor cells.

Proliferating cell nuclear antigen (PCNA), a proliferating cell nuclear antigen, plays an important role in the initiation of cell proliferation and is an indicator of cell proliferation. As shown in Figure 3F, PCNA was reduced after knocking down POLR2A in 786-O and 769-P cells. Consistently, the cyclin D1 and CDK4 proteins were decreased after knocking down POLR2A in 786-O and 769-P cells. The main function of cyclin D1 is to promote cell proliferation. Cyclin D1 binds to and activates CDK4, a cyclin-dependent kinase that is unique to the G1 period. These results suggest that POLR2A may lead to reduced expression of cyclin D1 and G1 arrest in renal cancer cells.

POLR2A knockdown crippled tumor growth in vivo

The cell cycle control effect of POLR2A in vivo was validated in the 786-O xenograft model. 8 nude mice were subcutaneously injected with 3×10^6 cultured 786-O (4 nude mice with control and 4 nude mice with shPOLR2A) cells. Figure 4A represents the whole animal experiment design. Figure 4B

showed tumor tissues were surgically excised from the nude mice. We weighted two groups tumor weight and analyzed, tumor weight was significantly decreased in 786-O shPOLR2A group (Figure 4C, $P < 0.01$). In the whole experiment, mice body weight in two groups were also increased slowly, and no difference in 786-O control group and 786-O shPOLR2A group (Figure 4D). Furthermore, we calculated tumor volume change between two group, the tumor volume decreased significantly in 786-O shPOLR2A group comparing with 786-O control group (Figure 4E, $P < 0.001$).

The above results suggested that silenced POLR2A can inhibit RCC tumor cell growth in vivo.

Discussion

In this study, we focused on POLR2A, a well-known mutation gene in human cancers[21, 22, 24]. *VHL* and *PBRM1* had mutation rates of up to approximately 85% and 40% in ccRCC[3], respectively. POLR2A was the most highly dysregulated gene, with a high betweenness value (PPI) and high closeness value (PPI), after *VHL* and *PBRM1* mutations in the top 100 differentially expressed genes in our analyzed results (Figure 1). We further characterized the bio-function of POLR2A, and our results showed that silencing POLR2A inhibited tumor cell growth in vitro and in vivo (Figure 3 and 4).

To the best of our knowledge, the role of POLR2A in ccRCC is poorly understood. It has been reported that POLR2A is essential for cell survival. Clark et al found that *POLR2A* alterations led to the dysregulation of key identity genes in meningeal development[22]. Consistent with the function of POLR2A, according to our results, POLR2A led to the dysregulation of key identity genes after *VHL* or *PBRM1* mutations in ccRCC (Figure 1), and our results showed that tumor cell related pathways: E2F, G2M, mTOR1, and MYC signaling activated pathways were all in response to POLR2A high expression (Figure 2).

VHL, *PBRM1*, *BAP1*, *SETD2*, *KDM5C*, *PIK3CA*, *PTEN*, *MTOR* and *TP53* are all recurrent mutations in ccRCC[27], and Sabine et al. has reported that *VHL*, *TP53* and *Rb1* deletion causes ccRCC in mice and allows the progression of ccRCC in mice[28]. Importantly, *POLR2A*, a neighboring gene of *TP53* (located within 200 kb), has been reported to effect *TP53* gene in many human cancers[23, 29, 30]. According to the literature, suppression of POLR2A inhibits human colorectal carcinoma cells and is associated with the loss of *TP53*, proliferation and tumorigenicity in a p53-independent manner[21]. Meanwhile, colorectal cancer cells with hemizygous loss of POLR2A were more vulnerable to POLR2A inhibition than unaltered normal cells[21].

Cyclin D–CDK4/6 accumulation allows entry into the cell cycle, otherwise preventing cell cycle exit[31]. Cyclin D1, CDK4, and PCNA were detected in 786-O and 769-P cells, decreased cyclin D1, CDK4, and PCNA protein amount were observed in shPOLR2A RCC cells (Figure 3E). Colony formation and xenograft animal results further support the inhibitory effect of POLR2A on the growth of RCC cells (Figure 3C, D, and Figure 5).

Indeed, α -amanitin, which specifically represses POLR2A, has been reported to selectively inhibit the proliferation, survival and tumorigenic potential of tumor cells[32]. Furthermore, the toxicity of amanitin can be overcome by the conjugation of α -amanitin with monoclonal antibodies (cell surface marker) or by coating it with nanoparticles, as reported by Yunhua. et al. and Jiangsheng. et al., respectively[23, 24]. Due to cyclin POLR2A oncogenic functions in RCC, these findings suggest that targeting POLR2A could regulated tumor cell cycle exist or entrance.

Conclusions

In summary, our study revealed that *POLR2A* was the key protein stimulating RCC malignancy after *VHL* and *PBRM1* mutations, and demonstrated that silenced *POLR2A* crippled cell viability and proliferation in vivo and in vitro. We anticipate that specific target inhibition of *POLR2A* will be a therapeutic approach for treating human cancers.

Abbreviations

PBRM1: Polybromo-1; RCC: renal cell carcinoma; ccRCC: clear cell RCC; *VHL*: Von Hippel-Lindau; mTOR: mammalian target of rapamycin; BAF180: BRG1-associated factor 180; PD-1: programmed cell death 1; PD-L1: programmed cell death 1 ligand 1; PCNA: Proliferating cell nuclear antigen.

Declarations

Acknowledgments

No.

Authors' contributions

Wang Kefeng, Wang Yao conceived and supervised the study;

Qiu Zhengguo, Zhang Xiaozhi and Wang Yao downloaded and interpreted the data;

Qiu Zhengguo, and Chai Linyan conducted and performed the experiments;

Chai Linyan wrote the manuscript;

Wang Kefeng edited the manuscript.

All the authors reviewed and approved the manuscript.

Funding

This work was supported by grants from the China National Natural Scientific Foundation (81972861) and the Shaanxi Province International Cooperation (2018KW-059).

Availability of data

The data used to support the findings of this study are included within the article and the supplementary information files (Table [X](#) and Table [X](#)).

Ethics approval and consent to participate

Not applicable.

Consent for publication

All the data generated or analyzed in this study are included in this article. Other data that are relevant to this article are available from the corresponding author upon reasonable request.

Competing interests

The authors declare that they have no competing interests.

References

1. Siegel RL, Miller KD, Jemal A. Cancer statistics, 2020. *CA Cancer J Clin.* 2020; 70: 7-30.
2. Moch H, Cubilla AL, Humphrey PA, Reuter VE, Ulbright TM. The 2016 WHO Classification of Tumours of the Urinary System and Male Genital Organs-Part A: Renal, Penile, and Testicular Tumours. *Eur Urol.* 2016; 70: 93-105.
3. Turajlic S, Swanton C, Boshoff C. Kidney cancer: The next decade. *J Exp Med.* 2018; 215: 2477-9.
4. Gossage L, Murtaza M, Slatter AF, Lichtenstein CP, Warren A, Haynes B, et al. Clinical and pathological impact of VHL, PBRM1, BAP1, SETD2, KDM6A, and JARID1c in clear cell renal cell carcinoma. *Genes Chromosomes Cancer.* 2014; 53: 38-51.
5. Piva F, Santoni M, Matrana MR, Satti S, Giulietti M, Occhipinti G, et al. BAP1, PBRM1 and SETD2 in clear-cell renal cell carcinoma: molecular diagnostics and possible targets for personalized therapies. *Expert Rev Mol Diagn.* 2015; 15: 1201-10.
6. Hogner A, Krause H, Jandrig B, Kasim M, Fuller TF, Schostak M, et al. PBRM1 and VHL expression correlate in human clear cell renal cell carcinoma with differential association with patient's overall survival. *Urol Oncol.* 2018; 36: 94 e1- e14.
7. Bihl S, Ohashi R, Moore AL, Ruschoff JH, Beisel C, Hermanns T, et al. Expression and Mutation Patterns of PBRM1, BAP1 and SETD2 Mirror Specific Evolutionary Subtypes in Clear Cell Renal Cell Carcinoma. *Neoplasia.* 2019; 21: 247-56.
8. Ricketts CJ, De Cubas AA, Fan H, Smith CC, Lang M, Reznik E, et al. The Cancer Genome Atlas Comprehensive Molecular Characterization of Renal Cell Carcinoma. *Cell Rep.* 2018; 23: 313-26 e5.
9. Young AC, Craven RA, Cohen D, Taylor C, Booth C, Harnden P, et al. Analysis of VHL Gene Alterations and their Relationship to Clinical Parameters in Sporadic Conventional Renal Cell Carcinoma. *Clin Cancer Res.* 2009; 15: 7582-92.
10. Pollard PJ, El-Bahrawy M, Poulosom R, Elia G, Killick P, Kelly G, et al. Expression of HIF-1alpha, HIF-2alpha (EPAS1), and their target genes in paraganglioma and pheochromocytoma with VHL and SDH mutations. *J Clin Endocrinol Metab.* 2006; 91: 4593-8.
11. Donovan EA, Kummar S. Targeting VEGF in cancer therapy. *Curr Probl Cancer.* 2006; 30: 7-32.
12. Nargund AM, Osmanbeyoglu HU, Cheng EH, Hsieh JJ. SWI/SNF tumor suppressor gene PBRM1/BAF180 in human clear cell kidney cancer. *Mol Cell Oncol.* 2017; 4: e1342747.

13. Espana-Agusti J, Warren A, Chew SK, Adams DJ, Matakidou A. Loss of PBRM1 rescues VHL dependent replication stress to promote renal carcinogenesis. *Nat Commun.* 2017; 8: 2026.
14. Xia W, Nagase S, Montia AG, Kalachikov SM, Keniry M, Su T, et al. BAF180 is a critical regulator of p21 induction and a tumor suppressor mutated in breast cancer. *Cancer Res.* 2008; 68: 1667-74.
15. Sekine I, Sato M, Sunaga N, Toyooka S, Peyton M, Parsons R, et al. The 3p21 candidate tumor suppressor gene BAF180 is normally expressed in human lung cancer. *Oncogene.* 2005; 24: 2735-8.
16. Mota STS, Vecchi L, Zóia MAP, Oliveira FM, Alves DA, Dornelas BC, et al. New Insights into the Role of Polybromo-1 in Prostate Cancer. *International Journal of Molecular Sciences.* 2019; 20: 2852.
17. Kapur P, Pena-Llopis S, Christie A, Zhrebker L, Pavia-Jimenez A, Rathmell WK, et al. Effects on survival of BAP1 and PBRM1 mutations in sporadic clear-cell renal-cell carcinoma: a retrospective analysis with independent validation. *Lancet Oncology.* 2013; 14: 159-67.
18. Miao D, Margolis CA, Gao W, Voss MH, Li W, Martini DJ, et al. Genomic correlates of response to immune checkpoint therapies in clear cell renal cell carcinoma. *Science.* 2018; 359: 801-6.
19. Pan D, Kobayashi A, Jiang P, de Andrade LF, Tay RE, Luoma AM, et al. A major chromatin regulator determines resistance of tumor cells to T cell-mediated killing. *Science.* 2018; 359: 770+.
20. Braun DA, Hou Y, Bakouny Z, Ficial M, Sant' Angelo M, Forman J, et al. Interplay of somatic alterations and immune infiltration modulates response to PD-1 blockade in advanced clear cell renal cell carcinoma. *Nature Medicine.* 2020; 26: 909-18.
21. Errico A. Colorectal cancer: POLR2A deletion with TP53 opens a window of opportunity for therapy. *Nat Rev Clin Oncol.* 2015; 12: 374.
22. Clark VE, Harmanci AS, Bai H, Youngblood MW, Lee TI, Baranoski JF, et al. Recurrent somatic mutations in POLR2A define a distinct subset of meningiomas. *Nat Genet.* 2016; 48: 1253-9.
23. Liu Y, Zhang X, Han C, Wan G, Huang X, Ivan C, et al. TP53 loss creates therapeutic vulnerability in colorectal cancer. *Nature.* 2015; 520: 697-701.
24. Xu J, Liu Y, Li Y, Wang H, Stewart S, Van der Jeught K, et al. Precise targeting of POLR2A as a therapeutic strategy for human triple negative breast cancer. *Nat Nanotechnol.* 2019; 14: 388-97.
25. Rai K, Akdemir KC, Kwong LN, Fiziev P, Wu CJ, Keung EZ, et al. Dual Roles of RNF2 in Melanoma Progression. *Cancer Discov.* 2015; 5: 1314-27.
26. Livak KJ, Schmittgen TD. Analysis of relative gene expression data using real-time quantitative PCR and the 2(-Delta Delta C(T)) Method. *Methods.* 2001; 25: 402-8.
27. Hakimi AA, Voss MH, Kuo F, Sanchez A, Liu M, Nixon BG, et al. Transcriptomic Profiling of the Tumor Microenvironment Reveals Distinct Subgroups of Clear Cell Renal Cell Cancer: Data from a Randomized Phase III Trial. *Cancer Discov.* 2019; 9: 510-25.
28. Harlander S, Schönenberger D, Toussaint NC, Prummer M, Catalano A, Brandt L, et al. Combined mutation in Vhl, Trp53 and Rb1 causes clear cell renal cell carcinoma in mice. *Nature Medicine.* 2017; 23: 869-77.

29. Bidon B, Iltis I, Semer M, Nagy Z, Larnicol A, Cribier A, et al. XPC is an RNA polymerase II cofactor recruiting ATAC to promoters by interacting with E2F1. *Nat Commun.* 2018; 9: 2610.
30. Limviphuvadh V, Tan CS, Konishi F, Jenjaroenpun P, Xiang JS, Kremenska Y, et al. Discovering novel SNPs that are correlated with patient outcome in a Singaporean cancer patient cohort treated with gemcitabine-based chemotherapy. *Bmc Cancer.* 2018; 18.
31. Matthews HK, Bertoli C, de Bruin RAM. Cell cycle control in cancer. *Nat Rev Mol Cell Biol.* 2021.
32. Frischknecht L, Britschgi C, Galliker P, Christinat Y, Vichalkovski A, Gstaiger M, et al. BRAF inhibition sensitizes melanoma cells to alpha-amanitin via decreased RNA polymerase II assembly. *Sci Rep.* 2019; 9: 7779.

Figures

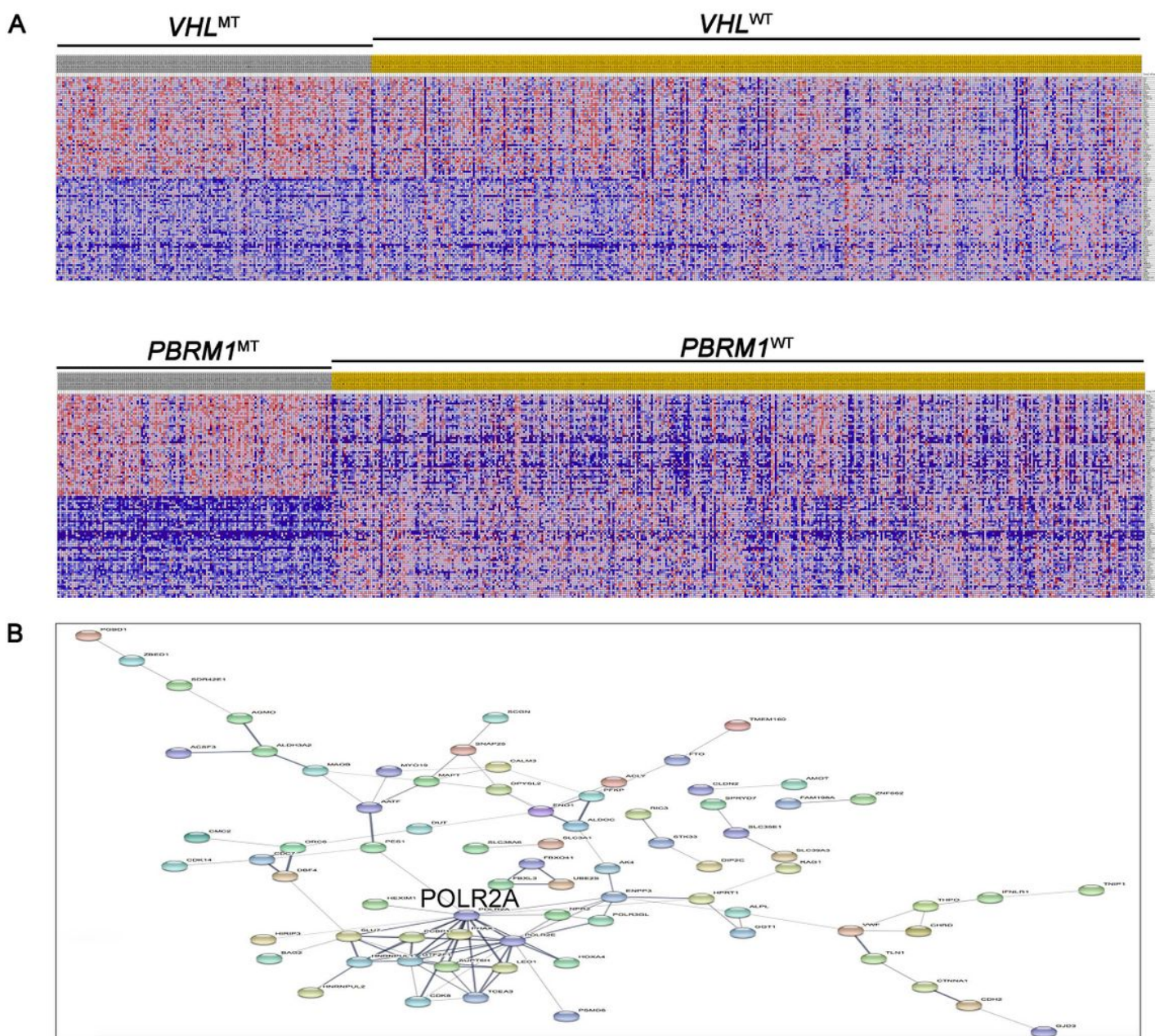


Figure 1

POLR2A is a hub gene following VHL and PBRM1 mutations in ccRCC. A Heat map of the top 100 significantly changed genes in patients with VHL and PBRM1 mutations compared to wild-type patients. Red indicates upregulated genes, and blue indicates downregulated genes. B The coexpression network showing the top 100 significantly changed genes in patients with VHL and PBRM1 mutations compared to wild-type patients. The network was constructed by STRING to investigate the PPI network.

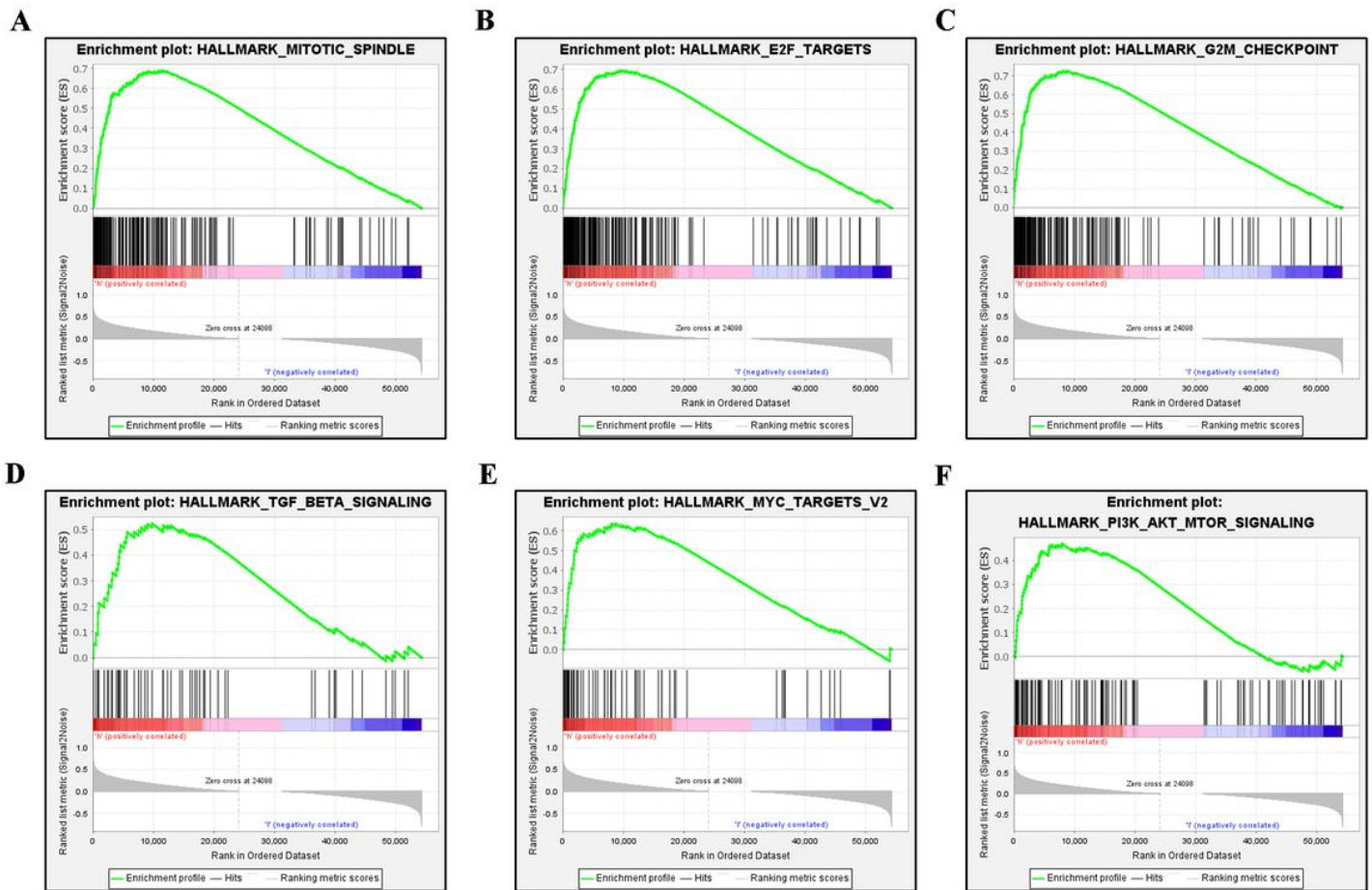


Figure 2

Significantly altered cell signaling pathways were response to increased POLR2A expression. A “HALLMARK_MITOTIC_SPINDLE”, Normalized Enrichment Score (NES) = 1.91, Nominal p-value = 0.0. B “HALLMARK_G2M_CHECKPOINT”, NES = 1.70, Nominal p-value = 0.01. C “HALLMARK_E2F_TARGET”, NES = 1.57, Nominal p-value = 0.06. D “HALLMARK_TGF_BETA_SIGNALING”, NES = 1.49, Nominal p-value = 0.06. E “HALLMARK_MYC_TARGETS_V2”, NES = 1.44, Nominal p-value = 0.14. F “HALLMARK_PI3K_AKT_MTOR_SIGNALING”, NES = 1.48, Nominal p-value = 0.04.

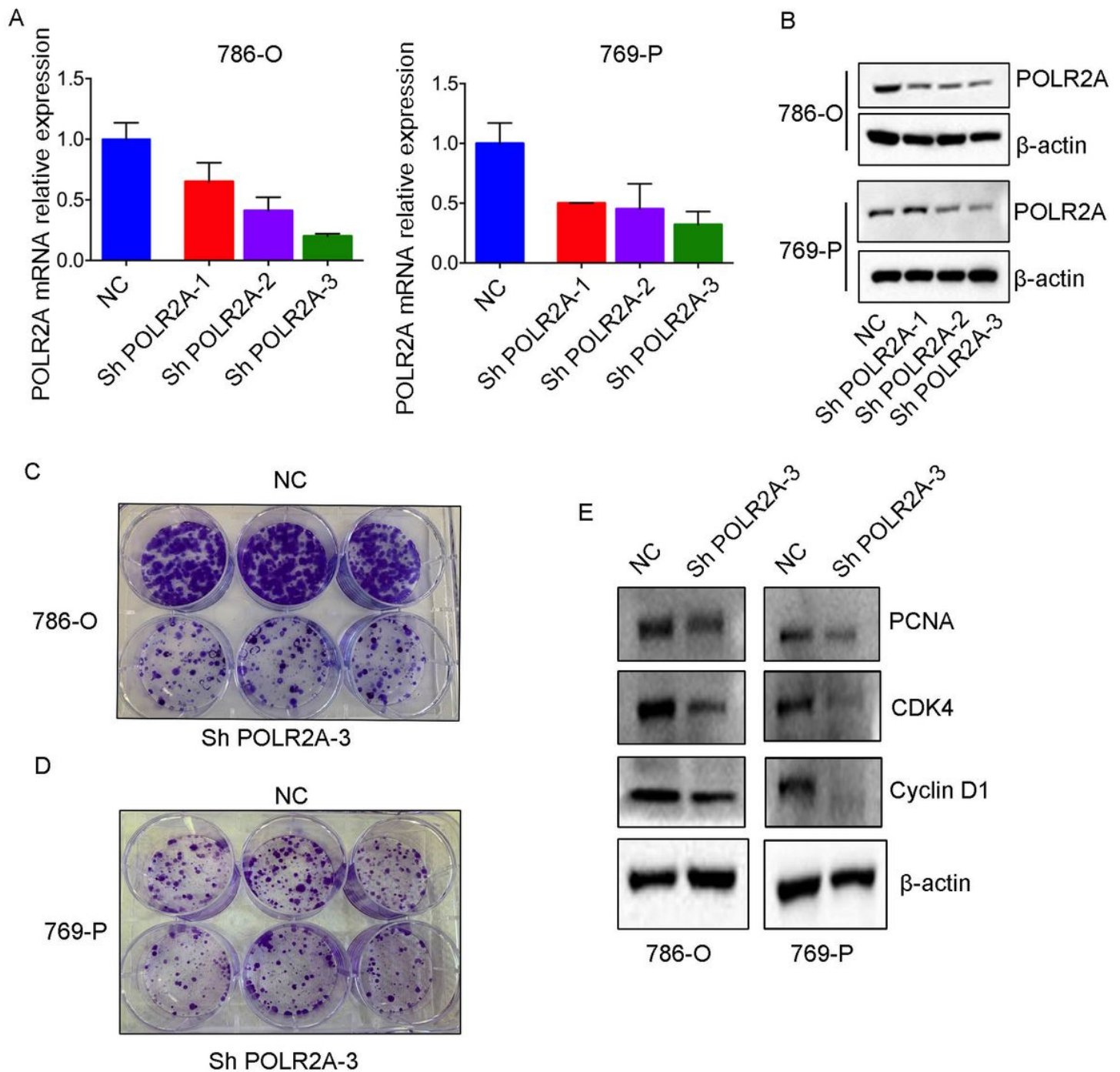


Figure 3

Knocking down POLR2A inhibits the growth of ccRCC cells. A Protein and mRNA POLR2A expression was detected by western blotting and qRT-PCR analysis. B, C Colony formation of ccRCC cells was performed in POLR2A-silenced (plasmid for knocking down POLR2A) or NC (negative control plasmid) 786-O and 769-P cells. Triplicates were performed in each experiment, and cells were visualized by crystal violet staining. D Knocking down POLR2A decreased cell cycle-related proteins in ccRCC cells. The cyclin D1, CDK4, and PCNA protein levels were detected in cell lysates in POLR2A-silenced (plasmid for knocking down POLR2A) or NC (negative control plasmid) 786-O and 769-P cells, respectively.

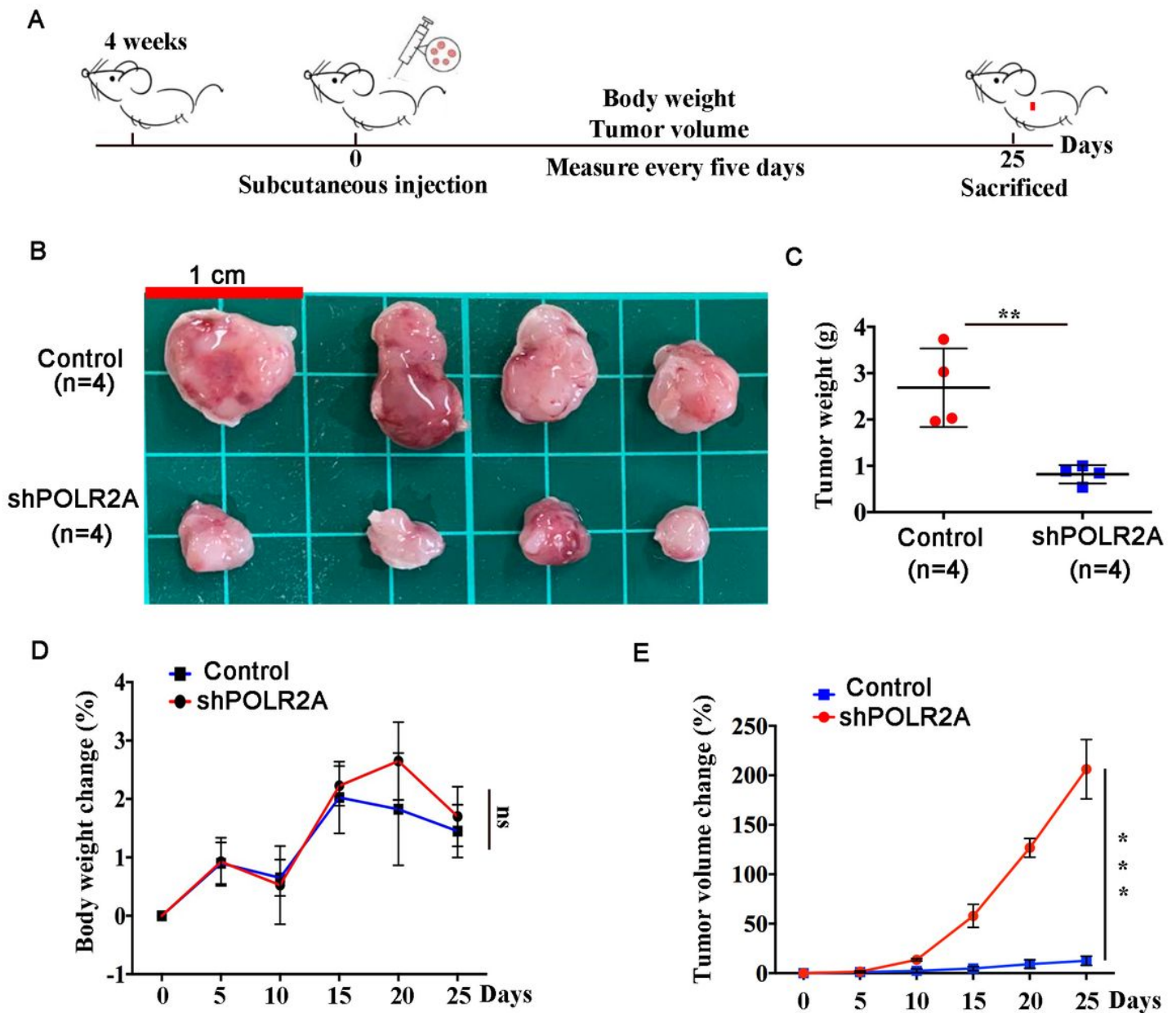


Figure 4

Knocking down POLR2A inhibits tumor growth in vivo. A Protocol for bearing BALB/c nude mice treatment in this study. B Tumor images from control and shPOLR2A groups. C Tumor weight of xenografted mice in control and shPOLR2A groups. D Body weight changes of the xenografted mice in control and shPOLR2A groups. E Tumor volume changes in the xenografted mice during control and shPOLR2A groups. Statistical analysis of the data was calculated using student's t test between two groups, error bars indicate \pm SD, n=4. **p<0.01 as compared with the control group, ***p<0.001 as compared with the control group, ns no significant.

Supplementary Files

This is a list of supplementary files associated with this preprint. Click to download.

- [supplementary.pdf](#)